

Analysis of Torque in Permanent Magnet Synchronous Motors with Fractional Slot Windings

J. A. Güemes¹, A. M. Iraolagoitia¹, M. P. Donsión² and J. I. Del Hoyo³

¹ Department of Electrical Engineering, University of Basque Country,
EUITI, Plaza de la Casilla 3, 48012 Bilbao (Spain)
joseantonio.guemes@ehu.es, ana.iraolagoitia@ehu.es

² Department of Electrical Engineering, University of Vigo
Campus of Lagoas Marcosende, 36310 Vigo (Spain)
IEEE, EA4EPQ and AEDIE member, donsion@uvigo.es

³ Department of Electrical Engineering, University of Basque Country,
ETSI, Alameda Urquijo s/n, 48013 Bilbao (Spain)
joseignacio.delhoyo@ehu.es

Abstract-The influence of various types of windings on the cogging torque and the total torque developed by a three-phase permanent magnet synchronous motor (PMSM) is investigated. The number of poles and rotor geometry are fixed and the stator slot number is modified. The finite element technique is used for the computation of the machine characteristic. The torque is determined by means of the Maxwell stress method. It is shown that the optimizing the cogging torque to a low value is therefore not sufficient to obtain a low torque ripple.

I. INTRODUCTION

Permanent magnet synchronous motors (PMSM) are widely used in many industrial applications for their compactness, highly efficient and high torque density. As their cost continues to decrease they have the opportunity to become a dominant force in the industrial applications market.

One of the most important problems in permanent magnet (PM) motors is the pulsating torque which is inherent in their design. This ripple is parasitic, and can lead to mechanical vibration, acoustic noise, and problems in drive systems [1]. The minimizing this ripple is of great importance in the design of PMSM [2]. The pulsating torque should be specially analyzed for the application of constant speed or high-precision position control, especially at low speed

Torque pulsations are due to the cogging torque and the electromagnetic torque ripple. The cogging torque is the consequence of the interaction between of the permanent magnets field and the stator slots, which produces reluctance variations with the rotor position, it is independent of stator current. The electromagnetic torque ripple is caused by the interaction of the stator magnetomotive force with the geometry and magnetic properties of the rotor [3].

In the literature, numerous methods for reducing the cogging torque, such as employing a fractional number of slots per pole, skewing of magnets and/or slots, displacing and shaping the magnets, optimizing the magnet pole-arc-to-pole-pitch ratio, introducing auxiliary slots or teeth etc, have been proposed [4]-[5].

The use of fractional number of slots per pole reduces the amplitude of the cogging torque but also increases the fundamental order (deformation of the waveform of the magnetic flux density in the air gap of the machine), since the stator slots are located at different relative circumferential positions with respect to the edges of the magnets. In general, the higher the least common multiple between the number of the poles and the number of slots stator, the lower the cogging torque.

The skew of magnets is effective in reducing the harmonic content in the flux linkage and back EMF waveform, as well as in reducing the cogging torque.

The main objective of the paper is to investigate the influence of several types of fractional slot windings on the cogging torque and torque ripple. The magnetic vector potential waveforms in the air gap are also obtained and compared.

II. MOTOR ANALYZED. TYPES OF WINDINGS

Three types of windings have been used for the analysis of 20-pole permanent magnet synchronous motor. The number of poles and rotor geometry are fixed and the stator slot number of stator slots is modified.

The cross section of 48 stator-slot PMSM, discussed in this paper is show in Fig. 1. Each rotor pole contains a magnet permanent type NdFeB that is magnetized across their shorter dimensions.

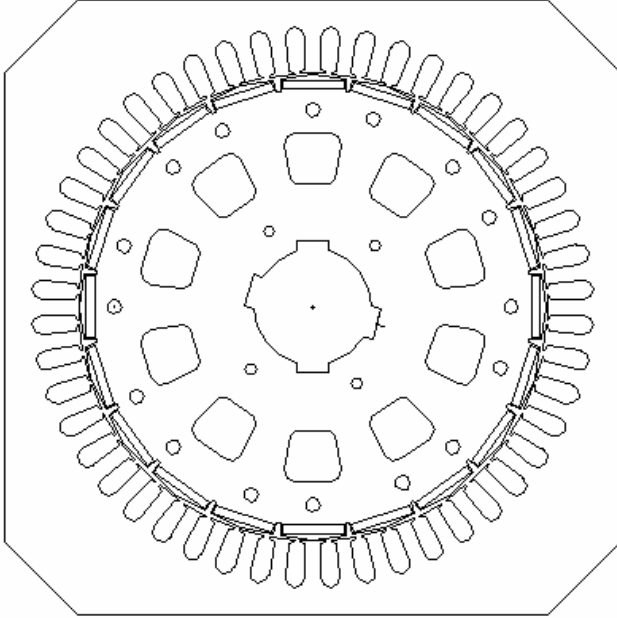


Fig. 1. Cross section of 48 stator-slot motor

Details of this machine are given in Table I.

TABLE I
DETAILS OF THE TEST MOTOR

Connection	Star
Controller device input voltage (line-to-line)	400 V
Frequency of the controller device input voltage	50 Hz
Frequency of the motor input voltage	15.5 Hz
Power rating (referred to 15.5 Hz)	3 kW
Current rating	10 A
Number of poles	20
Air-gap length	1 mm
Number of stator slots	48 - 24
Rotor outside diameter	318 mm
Stator inner diameter	320 mm
Shaft diameter	80 mm
Width of stator	420 mm
Permanent magnet material	NdFeB
Magnet thickness	5 mm
Width of magnet	42 mm
Coercive magnetizing intensity	922.5 kA/m
Remanent flux density	1.187 T

Figure 2 shows the diagrams of the windings used to investigate the influence on the cogging torque and torque ripple of the motor.

The three windings indicated, are fractional slot windings with a number of slots per pole and per phase “q” lower than unity. The last type is also called concentrated winding, because the coil is wound around one tooth.

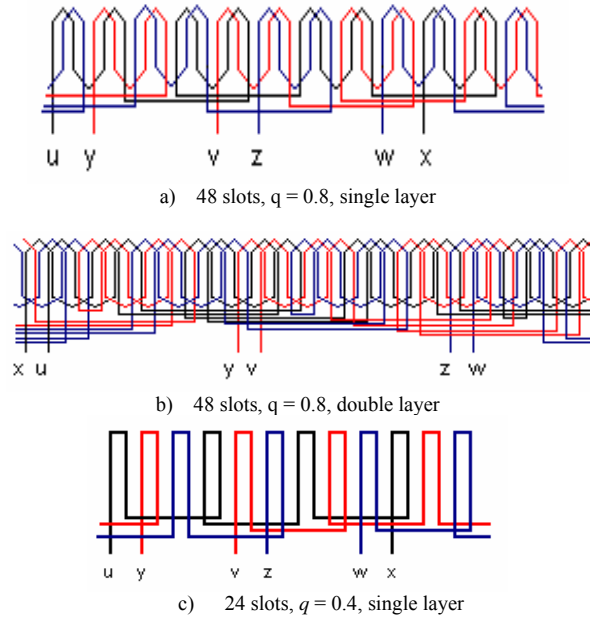


Fig. 2. Diagrams of fractional slot windings utilized

The number of periods of cogging torque waveform within the rotation of the one slot pitch depends on the combinations of poles number with slots number. So it is the ratio of poles number to the greatest common divisor (GCD) between the number of slots (K) and number of poles (2p) [6]. If it is high, de cogging torque is low.

$$n_p = \frac{2p}{GCD(K, 2p)} \quad (1)$$

Table II shows, number of slots, number of poles, greatest common divisor between slots number and poles number, number of periods of cogging torque (n_p), and slot pitch corresponding to windings analyzed.

TABLE II
NUMBER OF PERIODS OF COGGING TORQUE

K	2p	GCD	n _p	Slot pitch	Pole pitch
48	20	4	5	7,5°	18°
24	20	4	5	15°	18°

III. SIMULATION

The finite element technique is used for the computation of the machine characteristic. A non-linear field analysis is carried out for calculating the magnetic flux density in each one of the elements of the model.

The model utilized is constituted by a transverse section through the middle of the motor (360° geometry). The space of air surrounding the motor has to be taken into account too. The models of finite element method used are 2D plane.

The material property has been established as follows:

- For the air and copper (stator windings), by means of the magnetic permeability ($4\pi 10^{-7}$ H/m).

- For the lamination material of magnetic core, by means of its BH curve.
- For the permanent magnets by means of the coercive force and magnetic permeability (the second quadrant of the B-H characteristic of the permanent magnet utilized is linear)

The boundary condition is $A = 0$ (null magnetic vector potential) in the periphery of the model.

Figure 3 shows the finite element mesh used.

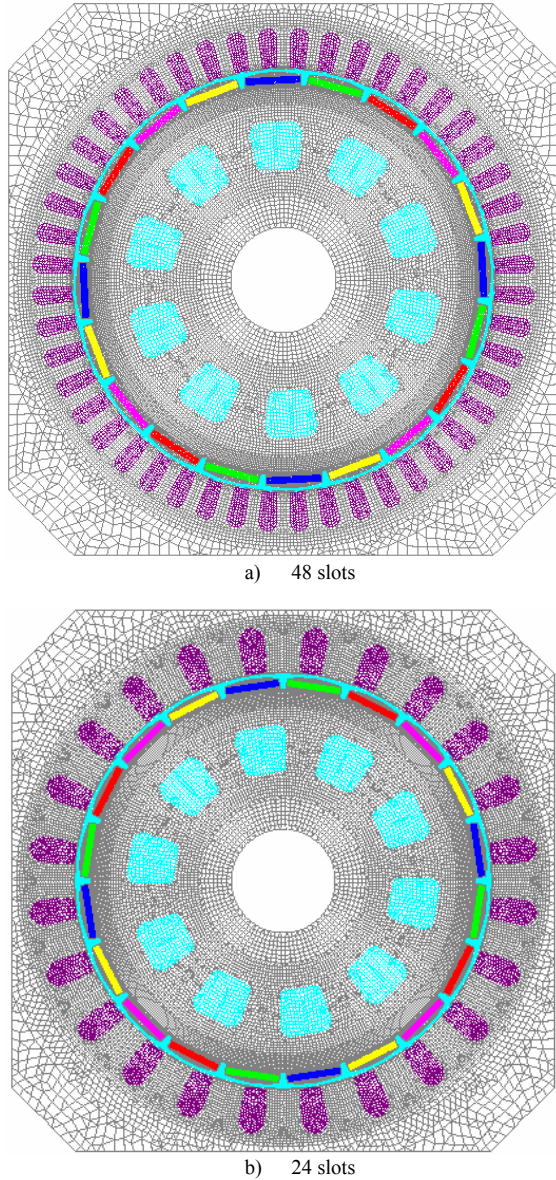


Fig. 3. Two-dimensional meshing model.

The cogging torque and torque ripple is calculated using the Maxwell stress method, with the equation [7]:

$$T = \frac{L}{\mu_0} \oint_l r B_n B_t dl \quad (2)$$

where L is stack length, l is integration contour, B_n is normal component of the magnetic flux density, B_t is tangential component of the magnetic flux density and r is the radius of the circumference which lies in the air gap.

To calculate the cogging torque the behaviour of the motor, for different position the rotor, when there is no current in the windings is simulated.

To calculate the electromagnetic torque, the load behaviour of the motor when the armature flux is perpendicular to excitation ($I_d = 0, I_q = I$), for different position of the rotor, is simulated.

IV. RESULTS

Figure 4 shows the air-gap magnetic vector potential waveforms obtained, once the analysis of the motors on no-load (without currents) have been carried out. We can observe that the air-gap magnetic flux density for the three analyzed winding is similar.

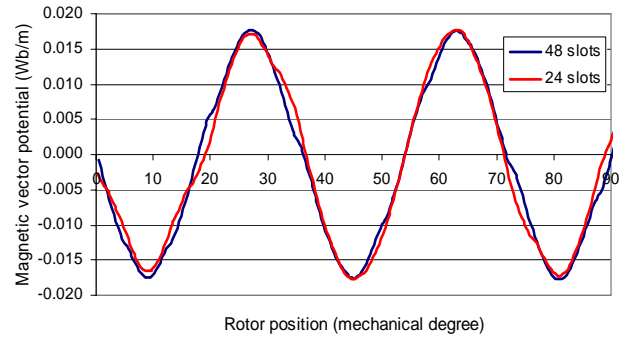


Fig. 4. Air-gap magnetic vector potential waveforms (without currents)

Figure 5 shows the air-gap magnetic vector potential waveforms obtained in the load analysis of the motors. As can be seen, the deformation of the waveform in the machine with 48 slots and double layer winding is lower than in the other machines.

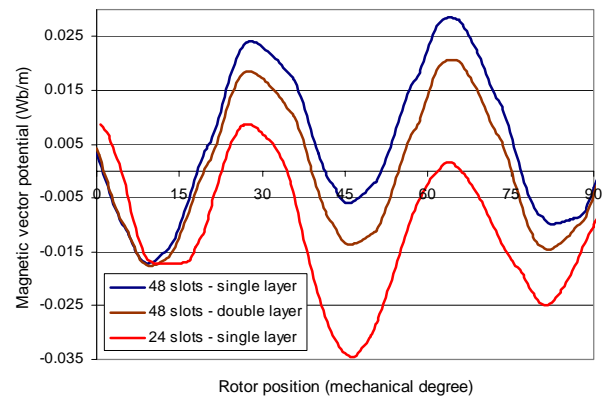


Fig. 5. Air-gap magnetic vector potential waveforms (load test).

Figure 6 shows cogging torque versus rotor position. The motor of 24 slots have lower cogging torque than the other machines analyzed.

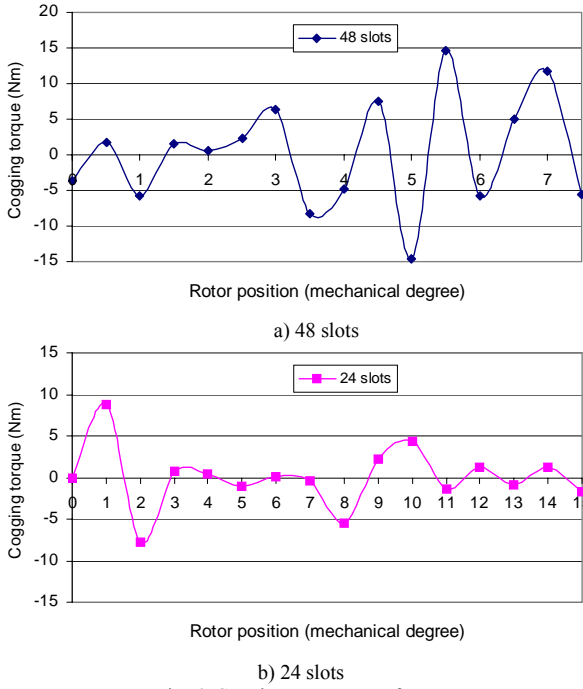


Fig. 6. Cogging torque waveforms.

Figure 7 shows electromagnetic torque versus rotor position.

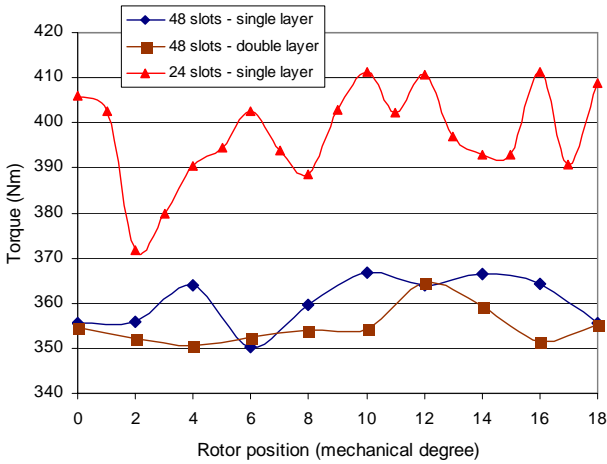


Fig. 7. Electromagnetic torque

The useful torque ripple factor (t_r) can be defined as following [8]:

$$t_r = \frac{T_{max} - T_{min}}{T_{av}} \cdot 100 \quad (3)$$

where T_{max} , T_{min} and T_{av} are, respectively, the maximal, minimal and average values of the torque

Table III shows the useful torque ripple factor for the three types of analyzed windings.

TABLE III
USEFUL TORQUE RIPPLE FACTOR

Number of slots and type of winding	T_{max}	T_{min}	T_{av}	T_r (%)
48 slots – single layer	367	350	360	4.58
48 slots – double layer	365	351	355	3.97
24 slots – single layer	411	372	397	9.96

Of the obtained results can be deduced:

- The average electromagnetic torque is higher in the machine of 24 slots.
- The 48-slot double-layer-winding machine has the lowest useful torque ripple factor.

V. CONCLUSIONS

Utilizing the finite element technique the influence of various types of windings on the cogging torque and torque developed by a PMSM has been investigated.

The deformation of the air-gap magnetic potential waveform in 48-slot double-layer-winding motor is lower than in the other machines.

The 24-slot motor has lower cogging torque than the 48-slot motors.

The 24-slot motor has average electromagnetic torque higher than the 48-slot motors.

The useful torque ripple factor (t_r) is minimum in the 48-slot double-layer-winding motor.

The torque ripple of the 48-slot motors is much lower than for the 24-slot machine. Optimising the cogging torque to a low value is therefore not sufficient to obtain a low torque ripple.

REFERENCES

- [1] L. Dosiek, and P. Pillay, "Cogging torque reduction in permanent magnet machines", *IEEE Industry Application*, vol. 43, no. 6, pp. 1656 – 1571, 2007.
- [2] Z.Q. Zhu, and D. Howe, "Influence of design parameters on Cogging torque in permanent magnet machines", *IEEE Trans. Energy Conversion*, vol. 15, no. 4, pp. 407-412, 2000.
- [3] R. Lateb, N. Takorabet, and F. Meibody-Tabar, "Effect of magnet segmentation on the Cogging torque in surface-mounted permanent-magnet motors", *IEEE Trans. Magnetics*, vol. 42, no. 3, pp.442-445, 2006
- [4] Z.Q. Zhu, S. Ruangsinchaiwanich, and D. Howe, "Synthesis of cogging-torque waveform form analysis of a single stator slot", *IEEE Trans. Industry Applications*, vol. 42, no. 3, pp. 650-657, 2006.
- [5] Salminen P., Pyrhönen J., Libert F., and Soulard J., "Torque Ripple of Permanent Magnet Machines with Concentrated Windings", ISEF 2005 - International Symposium on Electromagnetic Fields in Mechatronics, Electrical and Electronic Engineering, Baiona, Spain, 2005.
- [6] Xiuhé Wang, Yubo Yang, and Dajin Fu, "Study of cogging torque in surface-mounted permanent magnet motors with energy method", *Journal of Magnetism and Magnetic Materials* 267, pp. 80-85, 2003.
- [7] J.A. Güemes, "Finite Element Modeling of Permanent Magnet Synchronous Motors", Book of Abstracts ICEM 2002 – XV International Conference on Electrical Machines, Brugge, Belgium, 2002.
- [8] J.F. Gieras, and M. Wing, "Permanent Magnet Motor Technology. Design and applications". Marcel Dekker, Inc, New York, 2002.